Underground monitoring as the best way of roadways support design validation in a long time period

Piotr Małkowski[1]*✉ iD, Zbigniew Niedbalski[1]✉ iD, Tadeusz Majcherczyk[1]✉, Łukasz Bednarek[1]✉ iD

[1]AGH University of Science and Technology, Krakow, 30-059, Poland

*Corresponding author: e-mail malkgeom@agh.edu.pl, tel. +48126172104

Abstract

Purpose. The aim of this paper is to show the importance of geotechnical monitoring in assessing stability of an underground excavation. Every mining excavation is designed on the basis of limited geotechnical data and with some physical assumptions.

Methods. The monitoring in the brought up herein cases covered the rock mass and the support, and was carried out over a period of 6 years. Three long-term roadways in the hard coal mine, and with different support schemes, were studied. The monitoring methods included: convergence measurements, roof bed separation control, load on standing support and load on bolts.

Findings. The obtained results of the displacements of the roof rocks were highly affected by the type of the used support, roof stratification, and a rock strength. The more cracked and stratified were the roof rocks the stronger was the separation and the movement towards the excavation. The steel arch support sets with the bullflex bags lining can restrain this effect, but not the roof bolting with strand bolts grouted segmentally deep in the roof.

Originality. Rock mass and support monitoring of such a large scope, which was the subject of this research, is very seldom carried out in underground mining. Moreover, it was conducted over an exceptionally long period of six years. Five different techniques were used to assess the roadway's stability. Such a long-term monitoring and investigation allowed to find the relationships between the support scheme of the excavation and the rock mass movements around it.

Practical implications. A long-term monitoring allowed for a development of the deformation characteristics of the rock mass, defining the time of secondary equilibrium, and determination of the strain of the support elements. This, in turn, allowed for a verification of the correctness of selection of the support, installed in specific mining and geological conditions.

Keywords: rock mass monitoring, mining support monitoring, excavation stability, in-situ measurements, numerical modelling verification

1. The importance of monitoring in assessing stability of an underground excavation

Monitoring of excavations in natural conditions is one of the most important elements of optimisation of excavation design methods and support. On this basis, the excavation design can be verified in terms of its necessary dimensions, shape and lining method. The measurements of the behaviour of the excavation under given mining and geological conditions are the basis for performing a back analysis and verification of the adopted parameters of the physical model [1], [2]. Szwedzicki [3] indicates that rock cracking, loosening, spalling, and excavation convergence, as well as damage to the support, are always symptoms of loss of stability of the excavation.

Sedimentary rocks in roofs with interlayers are particularly susceptible to excessive separation [4]-[7], which most frequently occur in the vicinity of coal seams, and which are usually the cause of roof collapse. This type of roof rock should therefore be particularly observed. In addition, control studies of rock properties are carried out [8], [9], because their weathering or change of mining situation causes a change in their mechanical parameters [10]. This, in turn, leads to the weakening of the rock mass and a change of the strength factor in the rock mass. After some time, the stability of the excavation refers to the new geomechanical situation, different from the original design assumptions. Long-term monitoring is therefore essential for estimating the size of changes and the correctness of support selection.

The control of the behaviour of the roof and the floor of the excavation only, can be useful for the purpose of assessing the behaviour of the rock mass around the excavation [11]. Deformations of rocks are not always so visible as to enable an unambiguous assessment of the stability of the excavation and the correctness of the support selection. Therefore, in order to verify the design of underground excavations precise measurements of stress in the rock mass, displacement of rock strata or loads of the support are conducted [2], [12]-[15].

The most popular of these are measurements of roof separation or displacement, which are also the basis for the assessment of the risk of collapse, especially when rock bolting is used [4], [7], [16]-[19]. The second way to measure deformation is to assess the changes in the dimensions of the excavation, i.e. to measure convergence [2], [4], [9], [11]-[14], [19], [20]. A good way to assess fracture zones in the rocks around the excavation, in particular roof rocks, is to observe the walls of boreholes using a borehole endoscope [20]-[23].

The load measurements apply both to rock bolting and steel arch support. They provide relevant information about the strength factor of bolts [2], [7], [12] or the steel arch support construction [2], [4], [13], [14]. Stress changes in the rock mass and primary stress measurements for the verification of underground excavation designs are performed quite rarely, although they provide valuable information for proper rock mass and support modelling [16], [17], [24], [25].

During the modelling process, many different variants of support construction are usually analysed [26]-[32] and considering the intensive rock mass lamination as well [33]-[35]. Nevertheless, without feedback from the rock mass, i.e. conducting monitoring, correct calibration of the factors influencing the stability of the excavation is simply not possible. Many authors [1], [2], [36] emphasize that, without a properly pre-designed monitoring system, it is not possible to obtain valuable data for project verification and numerical re-calculation.

This article presents the results of tests on transport excavations of underground coal mines for a period of up to 6 years. They were performed by means of various measuring techniques including rock mass and support control. Such a long monitoring period allowed to develop the deformation characteristics of the rock mass, define the time of secondary equilibrium determination and the strength factor of support elements. This, in turn, allowed to verify the correctness of selection of the support, operating in specific mining and geological conditions.

2. Mining and geological conditions of the testing site

The tests of excavation stability were carried out in three different hard coal mines in Poland. They covered three excavations located at different depths, in varying geological conditions and with different support structures. All excavations were outside the influence of mining operations, being the main transport or ventilation excavations. The testing sites were located in the following excavations:

– Eastern roadway, depth – 1050 m;
– Ventilation drift W-1, depth – 950 m;
– Drift W, depth – 838 m.

In order to recognise the geomechanical properties of the rock strata around excavations, core boreholes were drilled in all measuring stations, from which samples for laboratory tests were taken. In the drilled boreholes, penetrometer tests were additionally carried out in order to determine *in situ* strength parameters of the rock strata. Subsequently, the boreholes were used for endoscopic testing.

The penetrometer tests consisted in pressing the penetrometer pin into the walls of the tested boreholes by means of oil pressure located in the hydraulic system of the device (Fig. 1). The indications of the manometer installed in the penetrometer supply pump determined the critical pressure at which the rock structure was damaged. At a given depth of the borehole, two measurements were taken, by means of rotating the head by 180°. On the basis of the obtained critical results of manometric pressures p_1 and p_2, the average manometric pressure p_{av} was determined. The penetrometer compressive strength was calculated from relationship (1):

$$\sigma_{c\,pen} = n \cdot p_{av}, \qquad (1)$$

where:

n – the constant of the penetrometer dependent on the type of head used: 1.18 or 1.80.

Figure 1. Hydraulic penetrometer

2.1. Eastern roadway

In the roof of the Eastern roadway, alternating strata of shale and sandy shale were deposited along the whole analysed length (Table 1). The thickness of the individual strata ranged from several dozen of centimetres to almost two metres. The strength of roof strata determined on the basis of penetrometer measurements was 40 MPa on average, and 70 MPa in laboratory conditions. The average value of the modulus of elasticity for the tested rocks was $E = 8.87$ GPa.

2.2. Ventilation drift W-1

Directly in the roof of Ventilation drift W-1 there was a 4-metre layer of shale, above which there was a coal seam (Table 2). Above, there were alternating strata of shale and mudstone. The strength of the roof determined in mining conditions was very low and amounted to 27 MPa, which was also half the strength specified in the laboratory on samples taken from the drill core ($\sigma_c = 52.95$ MPa). Such a large difference between the compressive strength values may be related to the low value of the Rock Quality Designation index ($RQD = 14.6\%$).

2.3. Drift W

Strata of sandy shale dominated in the roof of Drift W (Table 3). Directly in the roof of the excavation, there was a 4-metre thick layer of sandy shale, above which there was a layer of sandstone. The compressive strength of the roof strata tested by means of a penetrometer was about 41 MPa, while the compressive strength on the basis of laboratory tests was determined at 85 MPa. The tensile strength tested *in situ* and in the laboratory was $\sigma_{t\,pen} = 3.11$ MPa, $\sigma_{t\,lab} = 6.58$ MPa, respectively.

**Table 1. Geomechanical parameters in the roof of the Eastern roadway**

	Parameter	Value	Lithology in the borehole
$\sigma_{c\ lab}$	average [MPa]	70.25	
	standard deviation [MPa]	19.90	
	median [MPa]	68.38	
	coefficient of variation [%]	28.34	
$\sigma_{c\ pen}$	average [MPa]	40.52	
	standard deviation [MPa]	3.09	
	median [MPa]	42.19	
	coefficient of variation [%]	9.63	
$\sigma_{t\ lab}$	average [MPa]	7.09	
	standard deviation [MPa]	3.83	
	median [MPa]	5.93	
	coefficient of variation [%]	54.05	
$\sigma_{t\ pen}$	average [MPa]	2.70	
	standard deviation [MPa]	0.26	
	median [MPa]	2.81	
	coefficient of variation [%]	9.55	
E	average [MPa]	8.87	
	standard deviation [MPa]	1.55	
	median [MPa]	8.70	
	coefficient of variation [%]	17.43	
v [-]	average [-]	0.182	
	standard deviation [-]	0.079	
	median [-]	0.165	
	coefficient of variation [%]	43.93	
ρ	average [kg/m^3]	2671	
	standard deviation [kg/m^3]	47.34	
	median [kg/m^3]	2656	
	coefficient of variation [%]	1.77	
RQD	average [%]	43.7	
	range 0 ÷ 10 m [%]	0 – 92	

Table 2. Geomechanical parameters in the roof of Ventilation drift W-1

	Parameter	Value	Lithology in the borehole
$\sigma_{c\ lab}$	average [MPa]	52.95	
	standard deviation [MPa]	19.37	
	median [MPa]	61.96	
	coefficient of variation [%]	36.59	
$\sigma_{c\ pen}$	average [MPa]	27.87	
	standard deviation [MPa]	9.45	
	median [MPa]	29.55	
	coefficient of variation [%]	33.92	
$\sigma_{t\ lab}$	average [MPa]	4.68	
	standard deviation [MPa]	0.29	
	median [MPa]	4.68	
	coefficient of variation [%]	6.19	
$\sigma_{t\ pen}$	average [MPa]	1.98	
	standard deviation [MPa]	1.03	
	median [MPa]	2.19	
	coefficient of variation [%]	52.28	
E	average [MPa]	5.70	
	standard deviation [MPa]	2.08	
	median [MPa]	6.48	
	coefficient of variation [%]	36.48	
v [-]	average [-]	0.145	
	standard deviation [-]	0.045	
	median [-]	0.145	
	coefficient of variation [%]	31.03	
ρ	average [kg/m^3]	2735	
	standard deviation [kg/m^3]	75.64	
	median [kg/m^3]	2715	
	coefficient of variation [%]	2.76	
RQD	average [%]	14.60	
	range 0 ÷ 10 m [%]	0 – 53	

3

Table 3. Geomechanical parameters in roof strata of drift W

	Parameter	Value	Lithology in the borehole
$\sigma_{c\ lab}$	average [MPa]	85.31	
	standard deviation [MPa]	18.05	
	median [MPa]	85.76	
	coefficient of variation [%]	21.16	
$\sigma_{c\ pen}$	average [MPa]	41.26	
	standard deviation [MPa]	1.79	
	median [MPa]	41.13	
	coefficient of variation [%]	4.35	
$\sigma_{t\ lab}$	average [MPa]	6.58	
	standard deviation [MPa]	1.39	
	median [MPa]	6.87	
	coefficient of variation [%]	21.24	
$\sigma_{t\ pen}$	average [MPa]	3.11	
	standard deviation [MPa]	0.36	
	median [MPa]	3.05	
	coefficient of variation [%]	11.55	
E	average [MPa]	9.37	
	standard deviation [MPa]	0.60	
	median [MPa]	9.42	
	coefficient of variation [%]	6.40	
v [-]	average [-]	–	
	standard deviation [-]	–	
	median [-]	–	
	coefficient of variation [%]	–	
ρ	average [kg/m³]	2653	
	standard deviation [kg/m³]	54.01	
	median [kg/m³]	2634	
	coefficient of variation [%]	2.03	
RQD	average [%]	34.00	
	range $0 \div 10$ m [%]	71 – 100	

Sandy shale
Sandstone
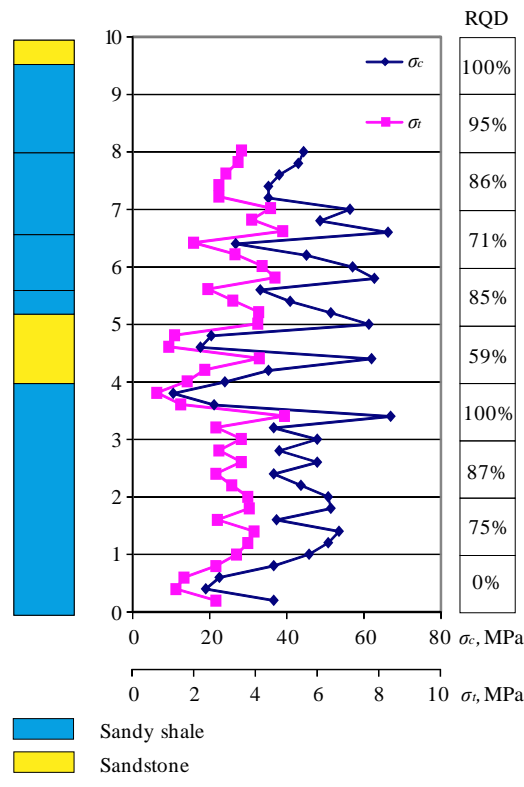
3. Numerical calculations and selection of excavation support

Based on the reconnaissance, prior to driving the excavation, support designs were made on the basis of numerical calculations. Predictions were made regarding stress distribution, the extent of crack zones and the displacement distribution. Calculations were made in the RS2 (formerly Phase2) program, using the Hoek-Brown failure criteria and the elastic-plastic model with associated flow plasticity theory. Parameters for the calculations were derived from the recognition of geomechanical properties, performed in the analysed area. Due to the variability of lithology on the excavation length, and at the same time the planned monitoring, the layout of rock layers was assumed as it was in the area of the designed measuring station.

3.1. Eastern roadway

The Eastern roadway was modelled in a several-meter layer of shale, with a thickness of 9.5 m (Fig. 2).

It was assumed that there is a thin layer of coal (0.25 m) in the roof, then a 7.5 m layer of sandy shale and a 3.5 m layer of shale, and then again a thick layer of sandy shale with thin layers of coal. A layer of shale (15.2 m) with a thin interlayer of coal was modelled in the floor. A layer of sandstone and sandy shale has been adopted below.

The results of numerical calculations indicate that the principal stress σ_1 assumes the highest values i.e. about 35 MPa at a distance of a few metres from the contour of the excavation in the sandy shale roof layer.
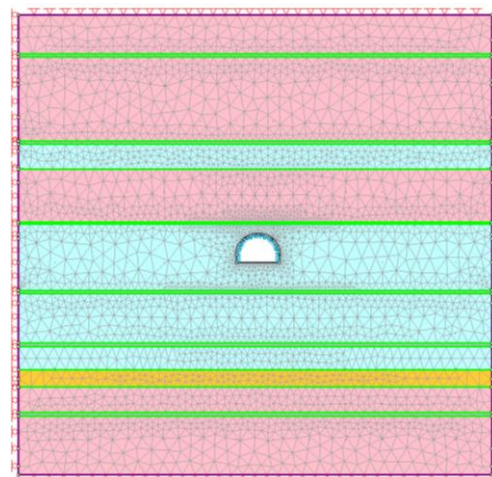
Figure 2. Numerical model of Eastern roadway

The map also shows the yielded zones, which indicate the possibility of a failure zone due to shear and tension in the vicinity of the excavation to a distance of about 2.0 m in the roof and about 4 m in the floor. A predicted shear failure zone may amount to 4-5 m in the sidewall and even 5-6 m in the floor (Fig. 3).

The predicted displacement around the analysed excavation indicates that there may be a floor upheaval of 0.3 m. For the remaining contour, the expected value is half smaller (Fig. 4).

Therefore, it can be concluded that the obtained values are rather small compared to those observed at a depth of about 1000 m.
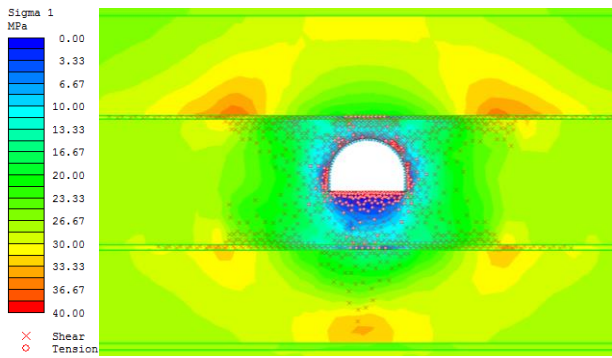
Figure 3. Principal stress distribution σ₁ together with the predicted yielded elements around the Eastern roadway
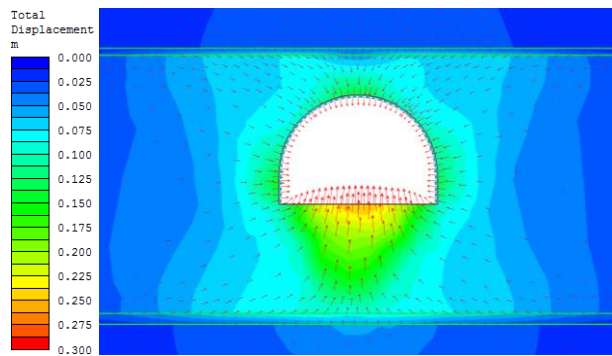

Figure 4. Total displacement distribution around the Eastern roadway

3.2. Ventilation drift W-1

On the basis of the recognition, similar calculations as for the Eastern roadway, were made before the Ventilation drift W-1 was driven. The excavation was modelled in a several-metre layer of shale (9.2 m – Figure 5). In the roof above, there are deposits of coal (2.0 m), sandy shale (2.0 m), and then alternating layers of shale, sandy shale and mudstone, which also contains a thin layer of coal (1.0 m). In the floor below the layer of shale, there is sandy shale (0.8 m), shale (1.0 m), coal (1.0 m) and again shale (3.5 m). Further, there are alternating layers of sandy shale, shale, coal and mudstone.
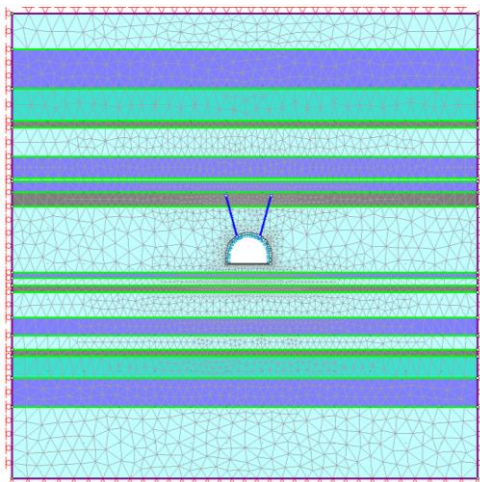

Figure 5. Numerical model of Ventilation drift W-1

The results of calculations indicate that the value of principal stress σ_1 is the highest in the shale layer and amounts to about 38 MPa at the distance of 3.0 meters from the excavation roof. The map also shows the yielded zones, which indicate the possibility of a failure zone due to shear and tension in the vicinity of the excavation, to a distance of about 0.5 m in the roof and sidewalls, and about 2-3 m in the floor. In the case of the predicted shear failure zone, it may amount to 2 m in the roof and the sidewall, and 4 m in the floor of the excavation (Fig. 6).
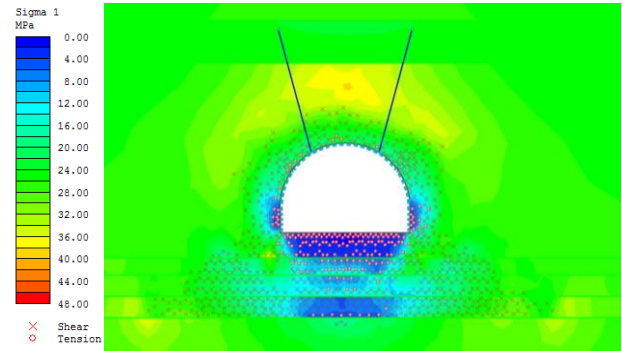

Figure 6. Principal stress distribution σ₁ together with the predicted yielded elements around Ventilation drift W-1

On the basis of the displacement map around the analysed excavation, it is possible to expect an upheaval of the floor in the range of about 0.13 m. On the contour of the excavation, the predicted displacement will be about 0.02-0.03 m (Fig. 7).
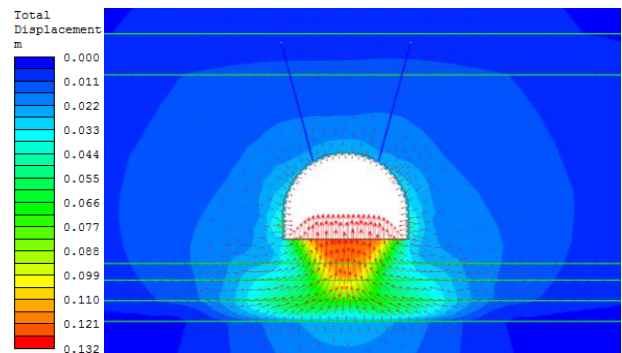

Figure 7. Distribution of total displacement around Ventilation drift W-1

3.3. Drift W

Drift W was modelled in a several-metre layer of sandy shale (12.5 m), whereas alternating layers of sandstone and sandy shale were adopted in the roof, which also contains a thin layer of coal (1.0 m) – Figure 8. In the floor below the layer of shale, it was assumed that there is sandy shale (3.5 m), then coal (1.5 m) and then sanded mudstone, sandstone and again sandy shale.

The results of the calculations indicate that principal stress σ_1 assumes the highest values of about 33 MPa at a distance of 4-5 meters from the floor of the excavation, i.e. at the point of contact of the sanded shale layer and the mudstone layer. The map also shows the yielded elements by shear and tension in the vicinity of the excavation, to a distance of about 0.5 m in the roof and sidewalls, and about 2 m in the floor.
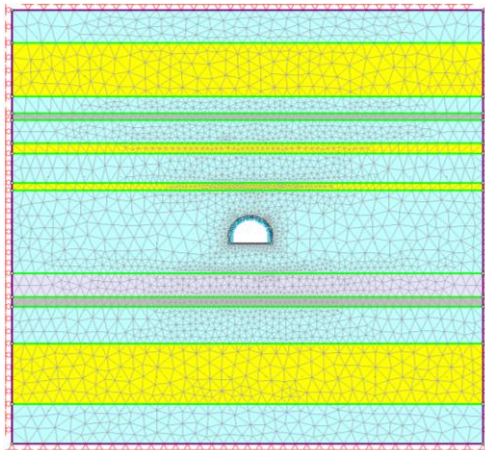
Figure 8. Numerical model of Drift W

In the case of the predicted shear failure zone, it may amount to 2 m in the roof and the sidewall, and 4 m in the floor of the excavation (Fig. 9).
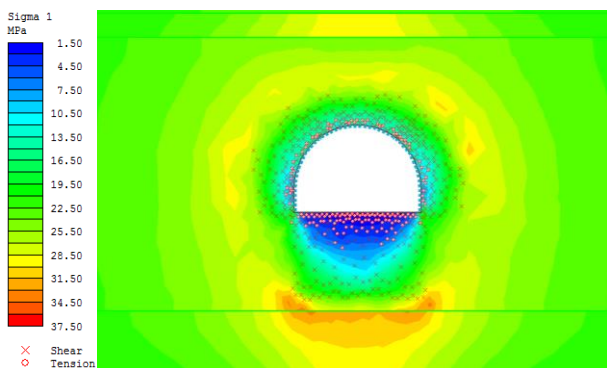

Figure 9. Principal stress distribution σ₁ together with the yielded elements around Drift W

The prediction of displacements around the analysed excavation indicates, that an upheaval of the floor of about 5 cm can be expected, as well as small 2-3 cm displacements around the perimeter of the excavation (Fig. 10). Therefore, it can be concluded that, from a practical point of view, the obtained values are negligible.
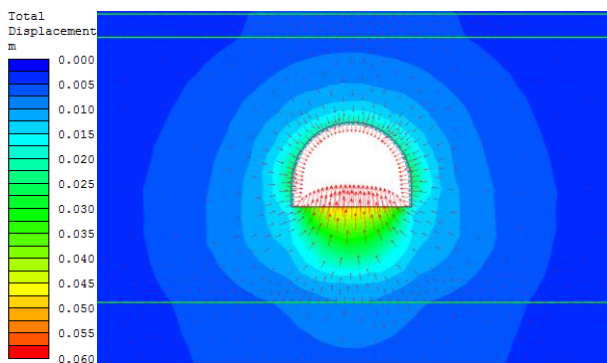

Figure 10. Distribution of total displacement around Drift W

3.4. Selection of support

On the basis of the obtained results of laboratory and mining tests and numerical calculations, the following types of support were used in the mentioned excavations:

– Eastern roadway – yielding steel arch support, 5.8 m wide and 4.025 m high (type LP11) with V32 profile (32 kg/1 m) made of S480W steel (yield point – 480 MPa) with spacing 0.5 m (working bearing capacity of the steel arch set – 650 kN), with bullflex bags with mineral-cement binder with the compressive strength of 40 MPa (Fig. 11);

– Ventilation drift W-1 – yielding steel arch support 6.1 m wide and 4.225 m high (type LP12) with V32 profile (32 kg/1 m) made of S480W steel (yield point – 480 MPa) with spacing 0.5 m (working bearing capacity of the steel arch set – 634 kN); additional reinforcement in the form of two steel anchored profile V beams fixed to the roof, with help of 6 meter long strand bolts (built about 2.4-2.8 m apart), and were installed every second field between the steel sets, in such a way that there was one bolt in each field (Fig. 12);

– Drift W – yielding steel arch support, 6.5 m wide and 4.225 m high (type LPCBor12), with profile V36 (36 kg/1 m) made of S550W steel (yield point – 550 MPa), with spacing 0.6 m (working bearing capacity of the steel arch set – 841 kN) (Fig. 13).

In order to protect against roof fall, a hook-on steel wire screen mesh is installed everywhere.

4. Measuring apparatus and methodology

In order to monitor the behaviour of the rock mass and its stability, a measuring station was built in each of the three excavations (Fig. 14).

The following measurements were carried out there:
– loads on steel sets support;
– displacement and separation of roof strata;
– bolt loads;
– fracturing of the surrounding rocks;
– changes in the dimension of the excavation.

The load measurement on the steel sets support was carried out using hydraulic dynamometers (Fig. 15). Two types of dynamometers were used: cylinder-shaped dynamometer (Fig. 16) and a three-point linear roof dynamometer. Foot dynamometers were placed under the rib arches and their task was to measure the load. The roof dynamometer was built on the roof arch in the arrow of the excavation to record the load coming from the roof strata.

Tests of roof strata separation performed using an extensometer consisted in introducing 18 measuring magnetic anchors into a borehole with a diameter of 42 mm and the length of 7.5 m (Fig. 17). The test was carried out by means of cyclic measurements, which provided information on the displacement of rock strata. Magnetic sensors were placed every 0.3 m to the height of 3 m of the borehole. Above 3 m from the excavation roof, they were positioned less densely, approx. every 0.5 m. Such positioning of measuring anchors was intended to precisely record separation and displacement of rock layers in the direct roof. The readings were taken by means of an extensometric probe, which recorded the position of a given measuring anchor in relation to the position of the base anchor.

To measure the rock bolt support load, an instrumented bolt was used (Fig. 17). Instrumented bolt was made of a standard anchor bolt modified for testing purposes. The bolt anchor modification consists in making two parallel grooves, in which tensometers are installed. The anchor length was 2.5 m, diameter 21.7 mm, while the tensometers, in the number of 9 pairs, were placed every 0.25 m from each other.
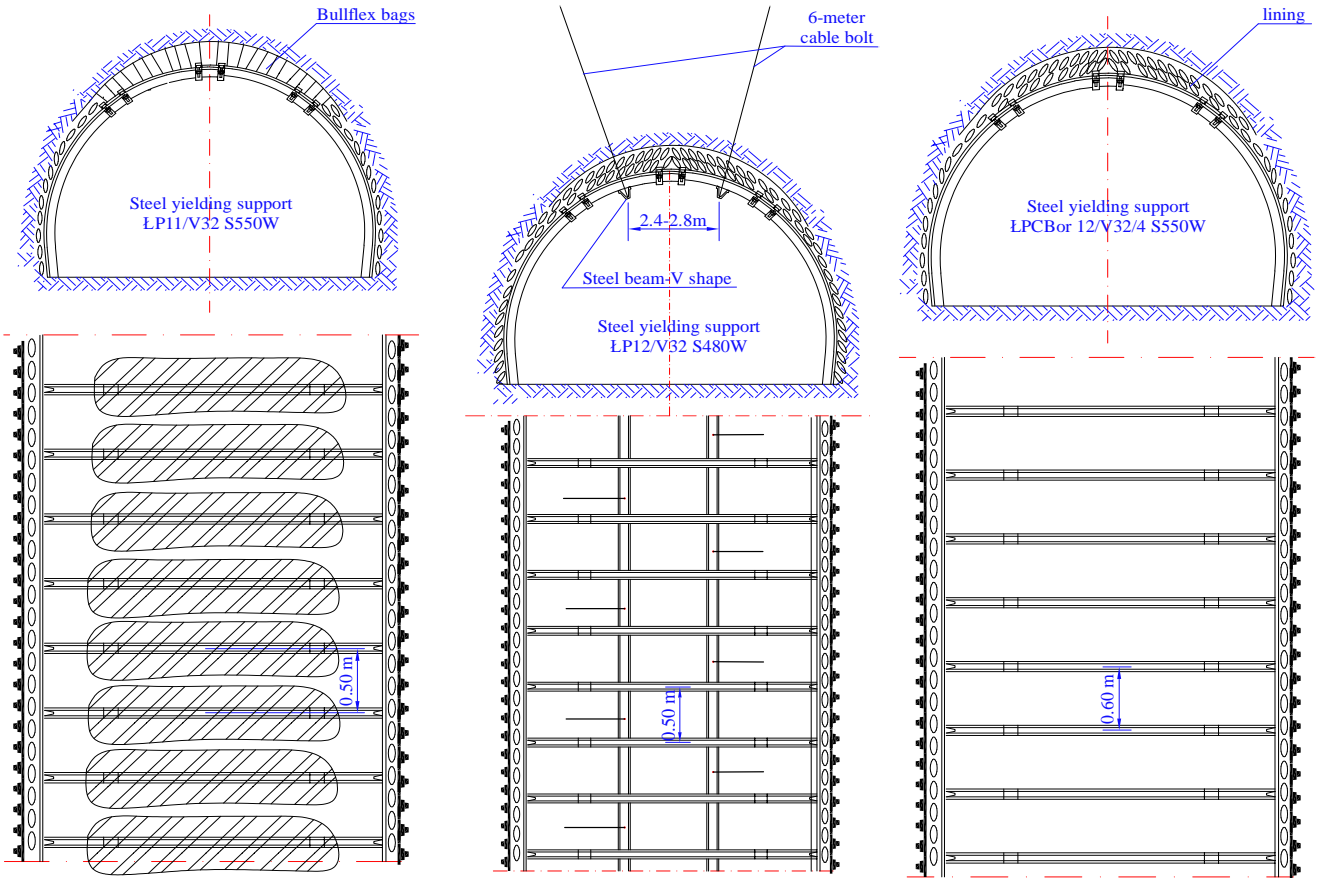
Figure 11. Support scheme in Eastern roadway

Figure 12. Support scheme in Ventilation drift W-1

Figure13. Support scheme in Drift W
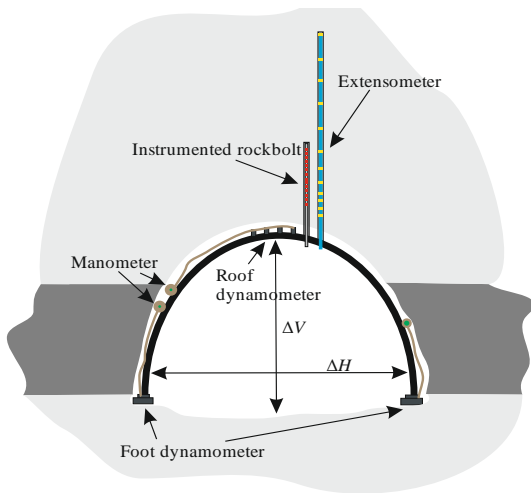
Figure 14. Measurement station

Figure 15. Hydraulic dynamometer

Figure 16. Measuring anchors of extensometric probe

Figure 17. Instrumented bolt – the groove fragment with tensometers attached

The anchor was made of steel with 640 MPa yield limit and 770 MPa tensile strength. Based on this, the maximum strength the steel can undergo at its elastic limit was determined to be 284 kN.

Endoscopic research involved consisted in recording discontinuities in the form of cracks and separation present in the rock mass around the excavation. In order to do this, an endoscopic camera was used and introduced into 95 mm diameter boreholes that had been used for penetrometer tests earlier. Its head with camera and infrared diodes is shown in the Figure 18.

Figure 18. Endoscopic camera head with infrared diodes

The changes in lateral dimensions of the excavation consisted in measuring height (ΔH) and width (ΔW) between fixed points constituting benchmarks (Fig. 14). The first measurement was a reference point for subsequent measurements and it was a base measurement. The change in height and width of the monitored excavation was measured by laser rangefinder or tape measure.

5. Monitoring of excavations

5.1. Eastern roadway

Eastern roadway was made as a main opening-out heading, through which a mine railway route is running. A bullflex bags filled with mineral-cement binding was used in the excavation. A measuring station in the Eastern roadway was made during the drilling at the 2372 meter. Monitoring with specialised equipment lasted for over 4 years. In the excavation there was no additional support e.g. in the form of rock bolts, thus the special attention was paid to measurements of steel arch support loads and displacements of roof layers.

Figure 19 shows the process of loads steel arch support recorded by hydraulic dynamometers under the ribs (foot dynamometers).
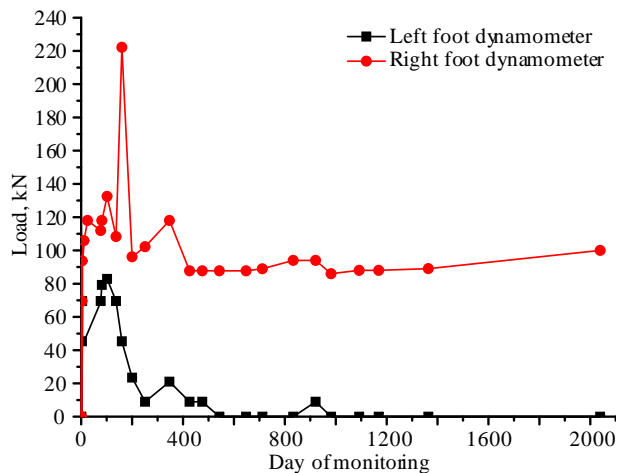

Figure 19. Set support load in the Eastern roadway

Unfortunately, the roof dynamometer, due to the inadequately bullflex bags, showed too low or zero values. Results analysis shows a very similar sidewall dynamometers qualitative process – they were loaded and unloaded simultaneously. However, the values of forces in the right sidewall (red colour) are significantly higher. Especially, at about 200th day of the measurement, there can be seen the highest load on right arch reaching 222 kN, therefore the support is loaded not evenly but mostly from the left side.

It should be noted that up until the 426th day of the measurement periodical support unloads occurred, i.e. probably the arch supports yielded under the load coming from roof rocks. A slight unload occurred also in the 882nd day of the measurement. However, it can be accepted that in this case the secondary loads formed for about 15 months. Then the loads were stabilised and it decreased to zero on the left side and on the right side it was about 90 kN.

Investigations carried out with a use of extensometric probe confirm the above observations. It can be seen that the most intense movement of roof rocks occurs before about 150th day from driving the excavation and the situation is practically stabilised in about 420th day of the monitoring (Fig. 20).
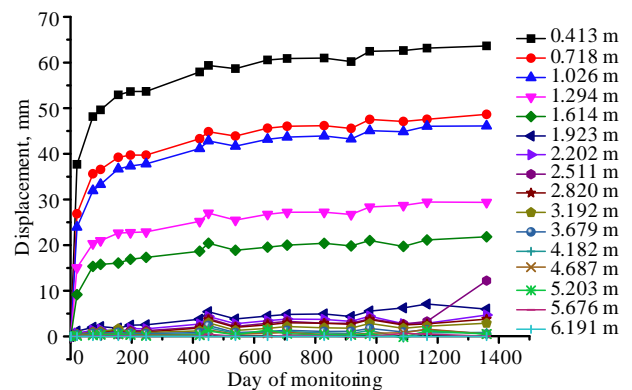

Figure 20. Roof strata displacement in the Eastern roadway

The most notable displacements of rock strata occurred in the direct roof of the excavation and they weaken as the distance from the excavation roof contour is growing. Additionally, the measurement proves that roof rocks move in packages, which is facilitated by their intense stratification (Table 1). At the depth of 0.4 m up the roof the displacements are approx. 60 mm, at the distance of 0.6-1.1 m – approx. 42 mm at the distance of 1.1-1.8 m – approx. 18-26 mm and above the strata they move a few millimetres. It should be noted that in the last day of the measurements the displacement of the measuring anchor installed at the depth of 2.51 m increased to 10 mm, which shows that another strata separated from the undisturbed rock mass and started to move downward.

In case of steel arch support without roof bolting the motion of rock strata occur continuously. The results of separation obtained with the extensometric probe were compared to the observed fracturing with the use of endoscopic camera (Fig. 21).

Endoscopic tests concern the first day of the measurements and the 644th day. i.e. the 22nd month after the excavation was driven. When analysing the results it can be seen that the area of cracks is growing in time, while the range of intense cracks stays at the level of 3.0 m, which is unchanged.
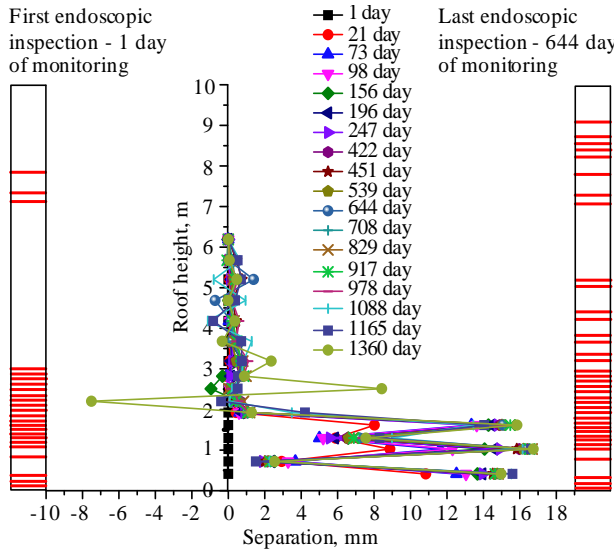
First endoscopic inspection - 1 day of monitoring

Last endoscopic inspection - 644 day of monitoring

Figure 21. A network of cracks and laminations in the Eastern roadway

However, there occurs the propagation of cracks up the roof and after 466 days they reached 5.1 m and the total range of cracks increased from 7.9 to 9.0 m. During this time, at the bottom part of the roof the displacements registered by extensometric probe increase slightly from 6-10 mm to 12-18 mm. In the 1360th day of the measurement displacement increased at the heights of 2.5 and 2.8 m, which results in subsequent cracks in roof rocks and subsequent propagation of the cracks. At the part of the roof where cracks and separation were significantly less numerous, that is beneath 4 m height, the anchors of the extensometric probe did not change their location during nearly the entire time of the observation. Such behaviour of the roof is determined by its lithology, because 12 rock beds were marked here together and they were shale and sandy shale.

5.2. Ventilation drift W-1

In the case of Ventilation drift W-1 the measurement have been carried out over the period of 5.5 years. Comparing the values of forces obtained in the dynamometers that control the load of the yield support (Fig. 22) it can be seen that here also the foot dynamometers are the most loaded ones.
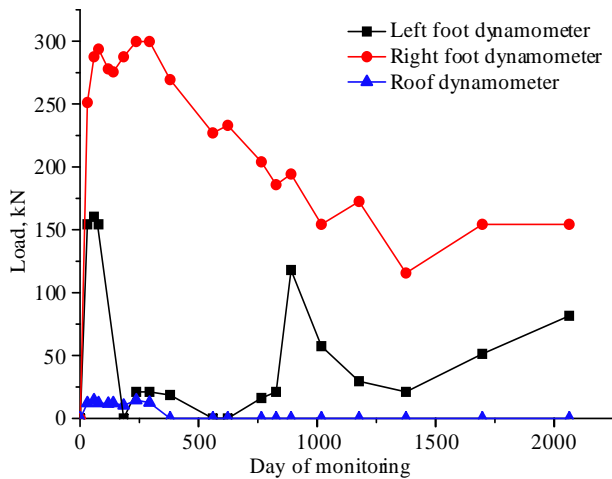

Figure 22. Support load in the Ventilation drift W-1

However, these values are higher and reach maximally 163 kN in the left sidewall and 300 kN in the right sidewall. The sum of the maximum load under the sidewall arches which is about 450 kN is lower than the maximum bearing capacity of the single steel set estimated to be 634 kN. However, it should be recalled that in this case the support was strengthened with steel beams, built in two rows along the excavation axis and anchored with strand bolts. Part of the load is therefore carried by these bolts. Bolting of the roof causes the load acting on a steel arch support to weaken in time, because a bolted rock beam is more rigid and deforms less.

Thus, within the period of approx. 420th days, the roof was unloaded entirely. Within the period of first 78th days, the value of the forces on both sidewall dynamometers is growing and before approx. 365th day it grows only on the right dynamometer. Cracked roof, after steel arch sets instalment, moved down, thus generating its load. In the next days, the load from the roof was resisted by support the standing, and additionally, by the bolts. Over time the steel arch sets was more loaded and more symmetric, however it cannot be stated that support load has been stabilised. Load vector is directed from the left side.

The installation of the bolts in Ventilation drift W-1 resulted in paying a special attention to the measurements from the instrumented bolt. In can be seen in the graph of the axial forces (Fig. 23) that the force in the bolt increases along with the depth.
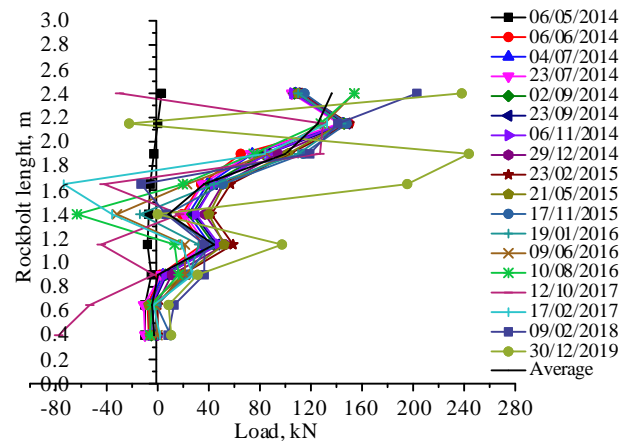
Figure 23. Axial forces in instrumented bolt – Ventilation drift W-1

In the initial period of the monitoring a constant image of the load could be seen: practically zero up to the height of approx. 0.9 m of the roof, and from 1.4 m a constant increase of the bolt load from 23 to 162 kN at the length of 2.2 m and approx. 112 kN at the end of its length, i. e. 2.5 m. Whereas the values of the loads along the bolt length increased slightly in time. Since June 2016 (the 25th month since the start of the monitoring), the loads acting on particular parts of the bolt begun to change drastically. On some of them the forces reached compressive values of 26-81 kN. This proves that roof beds loads periodically on the support and that they can be compacted. Latest measurements indicated further jumps in the values of the forces in particular tensometers of the bolt; ones that reached the guaranteed bearing capacity of the installed strand bolts 280 kN. Furthermore, the compaction of the rock beds are advancing up the excavation roof. Additionally, the black line indicates the curve that represents average bolt load on particular points from all taken measurements.

In relation to the above, the image of displacements of rock strata is slightly different. The measurements taken in the roof of the drift W-1 with the extensometric probe indicate that during 31 days the measuring anchors moved very quickly, yet the rock beds, also in a later period, moved only to a height of approx. 5.8 m (Fig. 24).
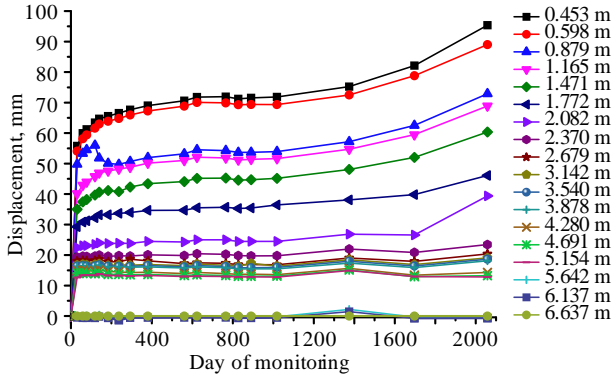

Figure 24. Displacement of rock beds in Ventilation drift W-1

Although the rock beds move in general in the direction of the excavation breakout the measuring course of the lines is vary. This proves that periodically rock beds movement towards the excavation is halted, because rock mass leans against the steel arch support sets. This takes place during a period between the 740th and 1020th day of the measurements, therefore at the same time when load on the steel arch support increased (Fig. 22). Similarly as in the Eastern roadway roof, the displacement of rock beds occurs in packages However, it is not so clear in this case, because Ventilation drift W-1 roof is not as strongly stratified as the roof of the former excavation. Furthermore, the 6.0 m long strand bolts installed in the roof were built with the rocks on the distance of approx. 1.6 m after ca. one month after the face driven, and their lower part may displace freely. Thus the lack of changes in the roof deformation in the area of grouting, i.e. 4.4 m and an insignificant one at the depth of 2.3-4.4 m. The changes took place only in the direct roof and here in the last 1000 days a package of rock beds moves down. This is reflected in the load on the anchor, as shown in Figure 23.

The displacements of roof rocks stabilised in the period of 620-1020 days, and at this time the maximum displacement of rocks in a package to the height of 0.7 m was approx. 72 mm. The registered displacement after 2096 days of the monitoring was 96 mm and a further movement of rock beds in the direction of the excavation may be expected.

5.3. Drift W

In the Drift W the measurements have been taken for 5.5 years. The results of load measurements on steel arch support setsindicate that the support was loaded stronger only to approx. 333rd day of the measurement (Fig. 25).

Although at that time small drops in the values of forces on the dynamometers were periodically observed. They reached the following values: on the sidewall dynamometers down to 96-98 kN on the roof dynamometer down to 145 kN, directly after the nearly steel support frames had been installed. Thus, for almost a year at the first the roof arch was loaded, then the forces were transmitted to the sidewall arches. After the 333rd day, the support was unloaded, as all three dynamometers indicated.
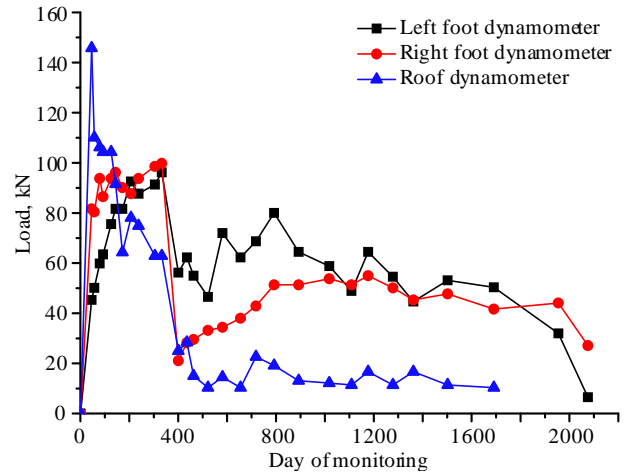

Figure 25. Steel arch support load in Drift W

The dynamometer under the left sidewall arch was slightly more loaded (up to 48-80 kN) in comparison to the rest of the dynamometers, although the slightest load could be observed in the roof dynamometer and it was approx. 10-20 kN. A local increase, by several kilonewtons in loads on dynamometers could be observed in the period of 700-800 days of the measurement and in the 1200 day. Thus, the read values allow to accept that after approx. 330 days the rock beds movement stabilised, and the subsequent presses resulted from the slight downward movement of rocks in the direction of the excavation. Furthermore, the support begun to be loaded more from the right side, which caused weaker load from the left side and from the roof. In the following days, the support was loaded especially from the roof side, and the yield structure caused the roof arch to be unloaded and the forces transmitted to on and under the sidewall arches. The roof dynamometer after the 1692nd day of the measurement was damaged.

The results of the measurements taken with the extensometric probe confirm, in general, the times in which the steel arch support sets loads occurred (Fig. 26).
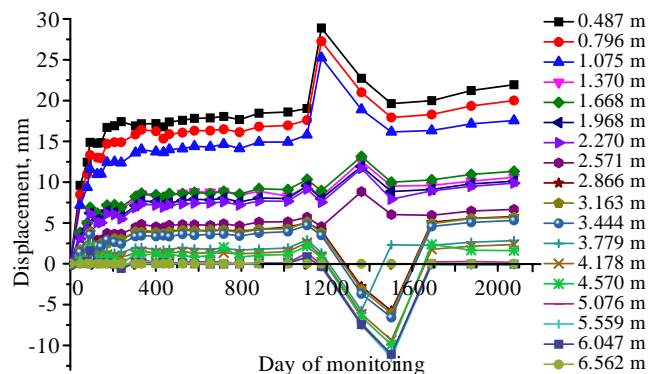
Figure 26. The displacement of rock strata in Drift W

Up to approx. 300th day of the measurement, they are the strongest roof displacement up to 17 mm. Until the 792nd day of the measurement there is no movement of the rock beds and in the 1175th day of the measurements there occurs a sudden movement of the nearly one meter strata of the direct roof. This displacement is approx. 12 mm. In the following days of the measurement the successive packages of rock beds moved sequentially: the part between 1.1 and 2.7 m downward and then the upper part between 2.7 and 6.5 m

upward. Thus, the roof plate was evening, which results in the packages of rock beds returning, to their positions from before the movement after the 1610th days. This behaviour suggests that the roof beds do not crack but move continuously.

It should be also noted that in case of Drift W the motion of the rock beds is significantly lesser in comparison to the excavations analysed before.

Here the direct roof displaced approx. 15-22 mm and the base roof 2-7 mm, whereas in case of the Eastern roadway it is 58-63 and 18-45 mm respectively and in case of the Ventilation drift W-1 – 70-90 mm and 15-40 mm. These slight roof displacements of the Drift W probably do not cause the cracking and breaking of rock beds, which are weakly stratified sandy shale.

Convergence measurement in Drift W was carried out on 5 bases over a distance of 100 meters, in the area of the measuring base (±50 m). Analysing the average changes in height and width, it can be concluded that convergence is still progressing, although measurements have been carried out for over 2000 days (Fig. 27).
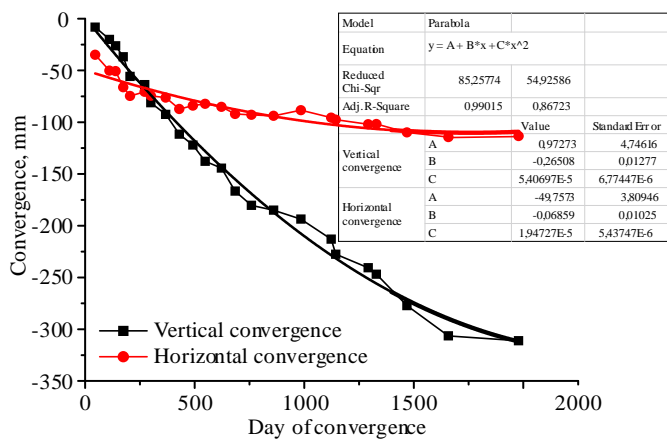

Figure 27. Change of width and height of Drift W

In the last measurement vertical convergence was found to be 311 mm and horizontal convergence – 114 mm. The intensity of horizontal convergence is therefore lower, but it has been found that some of the vertical deformations are related to the upheaval of the floor. Since the horizontal and vertical deformation process is arranged along certain curves over time, trend lines have been fitted to both processes. The logarithmic function and the quadratic polynomial were considered, because for both of them the value of *R-square* was approx. 90%. Ultimately, the quadratic function was selected, as its extremum could then be defined. The calculations show that the time that must elapse in Drift W conditions for convergence to reach the maximum values is 2585 days for vertical movements and 1715 days for horizontal movements. A mathematical description of the fitted trend lines is shown in Table 4.

Table 4. Fitting the trend line

Convergence	Function model	Fitting	Time for reaching the maximum value t_{max} [days]
Vertical	$K_V = 0.00005t^2 - 0.0686t - 49.76$	$R^2 = 87.8\%$	2585
Horizontal	$K_H = 0.00002t^2 - 0.2585t - 3.84$	$R^2 = 99.1\%$	1715

6. Conclusions and discussion

Each design of the excavation support should be verified. Although numerical methods are commonly used to select the support scheme, taking into account the layout of rock beds around the excavation and the variability of their properties, they also require many assumptions to be made, e.g. the primary stress regime or quantitative weakening of the rocks after failure in the failure criteria. Verification of the adopted models and consequently, of the adopted support schemes, can only be performed by monitoring. This monitoring must concern both the rock mass and the support. It should be stressed, that the rock mass movements in the excavation area are often asymmetric, local layers are laminated or wet. This results in asymmetric load of the support and periodic loosening of the roof strata. Therefore, only a simultaneous control of the behaviour of the rock mass and the support can indicate the proper interpretation of the occurring phenomena. The rock mass movements should be measured by means of controlling the excavation's convergence and the separation of rocks, especially roof rocks. The load measurement of the support should apply to each of the enclosed structures, in this case, the steel arch support sets and bolts. Measuring devices and techniques are very different and examples of measuring devices can be found e.g. on the manufacturers' websites [37]-[41].

During the monitoring of rock mass and support carried out in three selected main excavations located at the depths from 838 to 1050 m, convergence measurements, multilevel roof beds movements measured with an sonic extensometric probe, borehole endoscope, instrumented bolts and hydraulic dynamometers, were used. All these devices allowed to assess the performance characteristics of the support and to compare the results of predictions with the actual state.

Evaluating the selection of the support, it can be concluded that it was selected correctly, but with some reserve, because its bearing capacity in all cases was used in the range of 23-49%, referring to the maximum load values (sum of forces under the sidewall arches – Table 5). It was found however, that despite this, the support was subject to a certain yield displacement, which under laboratory conditions occurs at higher load values [42]. Therefore, it can be concluded that, on the one hand the spacing of the steel arch support sets is too small in long-term excavations, not affected by exploitation. In the analysed cases, it amounted to 0.5-0.6 m and could be increased. On the other hand, however, the technology of installing the steel yielding support in natural conditions did not allow to obtain the maximum bearing capacity.

Maximum displacements of the roof strata were estimated at a rather good level with the numerical models in case of the Eastern roadway and drift W, whereas in the Ventilation drift W-1 they are almost 3-times higher.

This could be a result of the high cracking of the roof beds found already at the recognition stage (RQD with zero value on the first 3 meters of the roof) and a too high initial assessment of the rock mass quality, used later in numerical calculations. At the same time, however, the predicted convergence of this excavation is rather precise and much higher than in the case of the rest of excavations.

It should be noted here that the obtained results of the displacements of the roof rocks are highly affected by the type of the used support and roof stratification and rock strength.

Table 5. Predicted and measured values of rock mass movements and support loads in selected excavations

Parameter		Eastern roadway	Ventilation drift W-1	Drift W
Burning depth [m]		1050	950	840
Steel arch support load [kN]	max. working bearing capacity of the single steel arch yielding set	650	914*	841
	sum of the max. forces under the sidewall arches	280	450	200
	average value of force over the entire period of the test	42	92.5	56.4
	percent of use of working bearing capacity	43	49	23
Displacement of the roof beds [mm]	maximum	122.9	95.4	17.4
	average	14.5	25.0	3.5
	predicted	115	35	20
Convergence [mm]	vertical	180	149	311
	predicted	375	160	90
	horizontal	161	38	114
	predicted	280	70	70
Roof separation [mm]	maximum	64.9	16.3	17.0
	average	3.8	3.9	1.6

*steel arch support with roof bolting

The most cracked and stratified among roof rocks in the Eastern roadway were the ones that separated and moved towards the excavation the most. However, the use of the steel arch support sets with the bullflex bags lining caused the transfer of loads to the support and, in effect, the limitation of the excavation convergence. The roof bolting with strand bolts grouted only on the 1.8 m section in the Ventilation drift W-1, didn't limit the beds separation in the roof and still allowed to move the rock beds downward. This was facilitated by a slightly lesser rocks strength and by the coal seam present in the roof at the 4-6 m distance. However, the essential part of the load was carried by the strand bolts there. The compressive strength over 90 MPa and little stratified roof rocks of the Drift W displaced insignificantly (17 mm) and separated insignificantly (17 mm). As was mentioned before, the vertical convergence concerned mainly the floor heaving. It should be stressed that no clear connection can be found between the depth burning of the excavation and the values read of monitored parameters.

In addition, an interesting observation was made when analysing Drift W convergence, where both the height and width changes of the excavation over time can be described with 90-percent accuracy by a quadratic function. The function shows, similarly to the rest of the measurements, that secondary state of stress in coal mines, disturbed by a long-term and multilevel exploitation form very long for the period of 5-7 years. Therefore, in case of mining excavation (e.g. gateways), there will occur their convergence, roof displacements, floor heaving and varying support loads for as long as the excavations are exploited.

In conclusion, it can be stated that multi-year testing of rock mass movements and support loads around main dog headings are a very good method of verifying the support used and project assumptions made about numerical models. By this method, a displacement of the support may be estimated, as well as time of forming secondary equilibrium of the rock mass and a characteristic of deformation of rocks in given mining-geological conditions may be determined. The measurements in the *in situ* conditions help also a calibration of parameters of the rock mass and of other conditions took into calculations (e. g. the state of stress and parameter of

failure criterion [9]). They also enable elaboration of statistical relationships and function of deformation trend of the rocks around the excavation. This in turn, allows to predict better the rock mass movements for next planned excavations.

Acknowledgements

References

[1] Feng, X.-T., & Hudson, J.A. (2010). Specifying the information required for rock mechanics modelling and rock engineering design. *International Journal of Rock Mechanics and Mining Sciences*, *47*(2), 179-194. https://doi.org/10.1016/j.ijrmms.2009.12.009

[2] Niedbalski, Z., Majcherczyk, T., & Małkowski, P. (2013). Monitoring of stand-and-roof-bolting support - design optimization. *Acta Geodynamica et Geomaterialia*, 215-226. https://doi.org/10.13168/agg.2013.0022

[3] Szwedzicki, T. (2003). Rock mass behaviour prior to failure. *International Journal of Rock Mechanics and Mining Sciences*, *40*(4), 573-584. https://doi.org/10.1016/s1365-1609(03)00023-6

[4] Jena, S.K., Ritesh, D.L., Manoj, P., & Kuldip, P. (2016). Analysis of strata controll monitoring in rground coal mine for apprehension of strata movement. *Proceedings of the Conference on Recent Advances in Rock Engineering (RARE 2016)*, 505-511. https://doi.org/10.2991/rare-16.2016.81

[5] Małkowski, P., Niedbalski, Z., & Majcherczyk, T. (2016). Investigations of hard coal mine roadways stability in stratified rock. *Ground Support 2016*. E. Nordlund, T.H. Jones and A. Eitzenberger (eds).

[6] Wu, G., Fang, X., Bai, H., Liang, M., & Hu, X. (2018). Optimization of roadway layout in ultra-close coal seams: A case study. *PLOS ONE*, *13*(11), e0207447. https://doi.org/10.1371/journal.pone.0207447

[7] Xie, Z., Zhang, N., Qian, D., Han, C., An, Y., & Wang, Y. (2018). Rapid excavation and stability control of deep roadways for an underground coal mine with high production in Inner Mongolia. *Sustainability*, *10*(4), 1160. https://doi.org/10.3390/su10041160

[8] Prusek, S., & Bock, S. (2008). Assessment of rock mass stresses and deformations around mine workings based on three-dimensional numerical modelling. *Archives of Mining Science*, *53*(3), 349-360.

[9] Małkowski, P., & Ostrowski, Ł. (2019). Convergence monitoring as a basis for numerical analysis of changes of rock-mass quality and Hoek-Brown failure criterion parameters due to longwall excavation. *Archives of Mining Sciences*, *64*(1), 93-118. https://doi.org/10.24425/ams.2019.126274

[10] Heidari, M., Momeni, A.A., & Naseri, F. (2013). New weathering classifications for granitic rocks based on geomechanical parameters. *Engineering Geology*, (166), 65-73. https://doi.org/10.1016/j.enggeo.2013.08.007

[11] Wang, C., Wang, Y., & Lu, S. (2000). Deformational behaviour of roadways in soft rocks in underground coal mines and principles for stability control. *International Journal of Rock Mechanics and Mining Sciences*, *37*(6), 937-946. https://doi.org/10.1016/s1365-1609(00)00026-5

[12] Singh, R., Singh, A.K., Mandal, P.K., Singh, M.K., & Sinha, A. (2004). Instrumentation and monitoring of strata movement during underground mining of coal. *Minetech*, *25*(5), 12-26.

[13] Majcherczyk, T., Małkowski, P., & Niedbalski, Z. (2011). Stand-and-roof-bolting support: an effective way of roadway reinforcement. *Proceedings of the 22nd World Mining Congress & Expo*, (1), 279-285.

[14] Majcherczyk, T., Niedbalski, Z., Małkowski, P., & Bednarek, Ł. (2014). Analysis of yielding steel arch support with rock bolts in mine roadways stability aspect. *Archives of Mining Sciences*, *59*(3), 641-654. https://doi.org/10.2478/amsc-2014-0045

[15] Szurgacz, D., & Brodny, J. (2019). Application of a roof support monitoring system for analysis of work parameters of a powered longwall system. *E3S Web of Conferences*, (105), 03022. https://doi.org/10.1051/e3sconf/201910503022

[16] Shen, B., King, A., & Guo, H. (2008). Displacement, stress and seismicity in roadway roofs during mining-induced failure. *International Journal of Rock Mechanics and Mining Sciences*, *45*(5), 672-688. https://doi.org/10.1016/j.ijrmms.2007.08.011

[17] Shen, B. (2013). Coal mine roadway stability in soft rock: A case study. *Rock Mechanics and Rock Engineering*, *47*(6), 2225-2238. https://doi.org/10.1007/s00603-013-0528-y

[18] Bigby, D., Mac, A.K., & Hurt, K. (2010). Innovations in mine roadway stability monitoring using dual height and remote reading electronic telltales. In *Materials of the 10th Underground Coal Operators' Conference* (pp. 145-160). Carlton, Victoria, Australia: University of Wollongong & the Australasian Institute of Mining and Metallurgy.

[19] Walke, D.V., & Yerpude, R.R. (2015). Significance of strata monitoring instruments in roof fall risk assessment of an underground coal mine. *International Journal of Scientific and Research Publications*, *5*(6), 1-8.

[20] Walentek, A. (2019). Analysis of the applicability of the convergence control method for gateroad design based on conducted underground investigations. *Archives of Mining Sciences*, *64*(4), 765-783. https://doi.org/10.24425/ams.2019.131065

[21] Majcherczyk, T., Małkowski, P., & Niedbalski, Z. (2005). Describing quality of rocks around underground headings: Endoscopic observations of fractures. *Eurock 2005 – Impact of Human Activity on the Geological Environment* (pp. 355-360). Konečny (ed). London, United Kingdom: Taylor and Francis Group.

[22] Małkowski, P., Niedbalski, Z., & Majcherczyk, T. (2008). Endoscopic method of rock mass quality evaluation – new experiences. In *Materials of the 42nd US Rock Mechanics Symposium and 2nd U.S.-Canada Rock Mechanics Symposium*. San Francisco, United State: American Rock Mechanics Association, ARMA 08-237.

[23] Walentek, A., Lubosik, Z., Prusek, S., & Masny, W. (2009). Numerical modelling of the range of rock fracture zone around gateroads on the basis of underground measurements results. *Proceedings of the 28th International Conference on Ground Control in Mining*, 121-128.

[24] Shen, B., Poulsen, B., Kelly, M., Nemcik, J., & Hanson, C. (2003). Roadway span stability in thick seam mining – field monitoring and numerical investigation at Moranbah North mine. In *Materials of the 2003 Coal Operators' Conference* (pp. 173-184). Carlton, Victoria, Australia: University of Wollongong, The AusIMM Illawarra Branch.

[25] Ptáček, J., Konicek, P., Staš, L., Waclawik, P., & Kukutsch, R. (2015). Rotation of principal axes and changes of stress due to mine-induced stresses. *Canadian Geotechnical Journal*, *52*(10), 1440-1447. https://doi.org/10.1139/cgj-2014-0364

[26] Mitri, H.S., & Hassani, F.P. (1990). Structural characteristics of coal mine steel arch supports. *International Journal of Rock Mechanics and Mining Sciences & Geomechanics Abstracts*, *27*(2), 121-127. https://doi.org/10.1016/0148-9062(90)94860-v

[27] Lendel, M. (2004). Rock bolting and rock support and their combination in hard coal mining – the comparative study made with UDEC. *Numerical modelling of discrete materials* (pp. 213-225). Konietzky (ed). London, United Kingdom: Taylor and Francis Group.

[28] Majcherczyk, T., & Niedbalski, Z. (2010). Numerical modeling used for designing of coal mine roadway support. *New Techniques and Technologies in Mining – Proceedings of the School of Underground Mining*, 77-82. https://doi.org/10.1201/b11329-14

[29] Bondarenko, V., Symanovych, G., & Koval, O. (2012). The mechanism of over-coal thin-layered massif deformation of weak rocks in a longwall. *Geomechanical Processes During Underground Mining*, 41-44. https://doi.org/10.1201/b13157-8

[30] Prusek, S., Rotkegel, M., & Witek, M. (2011). Comprehensive method for designing roadway supports. *Proceedings of the 22nd World Mining Congress & Expo*, (1), 223-232.

[31] Pivnyak, G., Bondarenko, V., Kovalevs'ka, I., & Illiashov, M. (2012). *Geomechanical Processes During Underground Mining*, 238p. Book. https://doi.org/10.1201/b13157

[32] Cała, M., Tajduś, A., Andrusikiewicz, W., Kowalski, M., Kolano, M., Stopkowicz, A., & Jakóbczyk, J. (2017). Long term analysis of deformations in salt mines: Kłodawa salt mine case study, Central Poland. *Archives of Mining Sciences*, *62*(3), 565-577. https://doi.org/10.1515/amsc-2017-0041

[33] Khalymendyk, I., & Baryshnikov, A. (2018). The mechanism of roadway deformation in conditions of laminated rocks. *Journal of Sustainable Mining*, *17*(2), 41-47. https://doi.org/10.1016/j.jsm.2018.03.004

[34] Małkowski, P. (2015). The impact of the physical model selection and rock mass stratification on the results of numerical calculations of the state of rock mass deformation around the roadways. *Tunnelling and Underground Space Technology*, (50), 365-375. https://doi.org/10.1016/j.tust.2015.08.004

[35] Kovalevska, I., Barabash, M., & Snihur, V. (2018). Development of a research methodology and analysis of the stress state of a parting under the joint and downward mining of coal seams. *Mining of Mineral Deposits*, *12*(1), 76-84. https://doi.org/10.15407/mining12.01.076

[36] Małkowski, P. (2017). Zarządzanie monitoringiem zagrożeń w górnictwie (Management of mining monitoring systems). *Inżynieria Mineralna*, *XVIII*(2), 215-224, https://doi.org/10.29227/IM-2017-02-24

[37] *Firma "DARKOP" CORPORATION Spółka z o.o.* [online]. Retrieved from http://darkop.com.pl/

[38] *ESS Earth Sciences*. [online]. Retrieved from http://www.esands.com

[39] *GEOKON*. [online]. Retrieved from www.geokon.com

[40] *Geosystems*. [online]. Retrieved from http://geosystems.com.au/

[41] *The RST Instruments*. [online]. Retrieved from https://rstinstruments.com/

[42] Rotkegel, M. (2013). ŁPw steel arch support – designing and test results. *Journal of Sustainable Mining*, *12*(1), 34-40. https://doi.org/10.7424/jsm130107

Підземний моніторинг як найбільш ефективний спосіб оцінки конструкції кріплення виробки в довгостроковій перспективі

П. Малковскі, З. Недбальскі, Т. Майхерчик, Л. Беднарек

Мета. Проведення комплексного геотехнічного моніторингу для оцінки стійкості підземної гірничої виробки у складних умовах з обмеженою кількістю геотехнічних даних і певним фізичними припущеннями.

Методика. Проведено моніторинг стану гірського масиву і кріплення виробки протягом 6 років. Були вивчені 3 виробки кам'яновугільної шахти різних конструкцій, які довгий час перебували в експлуатації. Методи моніторингу включали: вимірювання осідання, контроль за відстанню між покрівлею і підошвою, вимір навантаження на вертикальні опори і на кріплення. Використовувалося наступне обладнання: ендоскопічна камера, акустичні екстензометри, кріплення з вмонтованою вимірювальною апаратурою та гідравлічні динамометри.

Результати. Встановлено, що зміщення порід покрівлі у значній мірі визначається типом використовуваного кріплення, розшаруванням і міцністю порід покрівлі. Зі збільшенням тріщинуватості та шаруватості порід покрівлі сильніше проявляється розшарування пласта й переміщення порід у напрямку виробки. Визначено, що сталеві арочні кріпильні стійки, амортизовані надувними мішками Bullflex, пом'якшують вищевказаний ефект, при цьому анкерне кріплення не дає подібного результату. Підтверджено ефективність опорної конструкції обраного типу кріплення з урахуванням межі безпеки, а її несуча здатність у всіх випадках була 23-49%. Аналіз збіжності показав, що зміни за висотою і шириною виробки в часі можуть бути описані з точністю до 90% квадратичною функцією.

Наукова новизна. Встановлено взаємозв'язок між схемою кріплення виробки і рухливістю навколишнього її породного масиву, що дозволило дати кількісно-якісну оцінку стійкості виробки на підставі вельми тривалого 6-річного геотехнічного моніторингу.

Практична значимість. Отримані характеристики деформацій породного масиву, час вторинної рівноваги і напружень елементів кріплення в результаті довготривалого моніторингу підтвердили правильність вибору типу кріплення. Результати моніторингу корисні для зворотного аналізу фізичної моделі та прийнятих в ній параметрів, які згодом можуть використовуватися для побудови чисельної моделі.

Ключові слова: моніторинг породного масиву, моніторинг шахтного кріплення, стійкість виробки, натурні вимірювання, перевірка чисельним моделюванням

Подземный мониторинг как наиболее эффективный способ оценки конструкции крепи выработки в долгосрочной перспективе

П. Малковски, З. Недбальски, Т. Майхерчик, Л. Беднарек

Цель. Проведение комплексного геотехнического мониторинга для оценки устойчивости подземной горной выработки в сложных условиях с ограниченным количеством геотехнических данных и определенным физическими допущениями.

Методика. Проведено мониторинг состояния горного массива и крепления выработки в течение 6 лет. Были изучены 3 выработки каменноугольной шахты различных конструкций, которые долгое время находились в эксплуатации. Методы мониторинга включали: измерения оседания, контроль за расстоянием между кровлей и почвой, измерение нагрузки на вертикальные опоры и на крепь. Использовалось следующее оборудование: эндоскопическая камера, акустические экстензометры, крепь с вмонтированной измерительной аппаратурой и гидравлические динамометры.

Результаты. Установлено, что смещение пород кровли в значительной степени определяется типом используемой крепи, расслоением и прочностью пород кровли. С увеличением трещиноватости и слоистости пород кровли сильнее проявляется расслаивание пласта и подвижка пород в направлении выработки. Определено, что стальные арочные крепежные стойки, амортизированные надувными мешками Bullflex, смягчают вышеуказанный эффект, при этом анкерное крепление не дает подобного результата. Подтверждена эффективность опорной конструкции выбранного типа крепи с учетом предела безопасности, а ее несущая способность во всех случаях была 23-49%. Анализ сходимости показал, что изменения по высоте и ширине выработки во времени могут быть описаны с точностью до 90% квадратичной функцией.

Научная новизна. Установлена взаимосвязь между схемой крепи выработки и подвижностью окружающего ее породного массива, что позволило дать количественно-качественную оценку устойчивости выработки на основании весьма длительного 6-летнего геотехнического мониторинга.

Практическая значимость. Полученные характеристики деформаций породного массива, время вторичного равновесия и напряжения элементов крепи в результате долговременного мониторинга подтвердили правильность выбора типа крепи. Результаты мониторинга полезны для обратного анализа физической модели и принятых в ней параметров, которые впоследствии могут использоваться для построения численной модели.

Ключевые слова: мониторинг породного массива, мониторинг шахтной крепи, устойчивость выработки, натурные измерения, проверка численным моделированием